Supplement to: Transient evolution of the relative size distribution of earthquakes as a risk indicator for induced seismicity

Vanille A. Ritz, Antonio P. Rinaldi, Stefan Wiemer
Swiss Seismological Service at ETH Zürich, Zürich, Switzerland

Complement to Figure 1-b

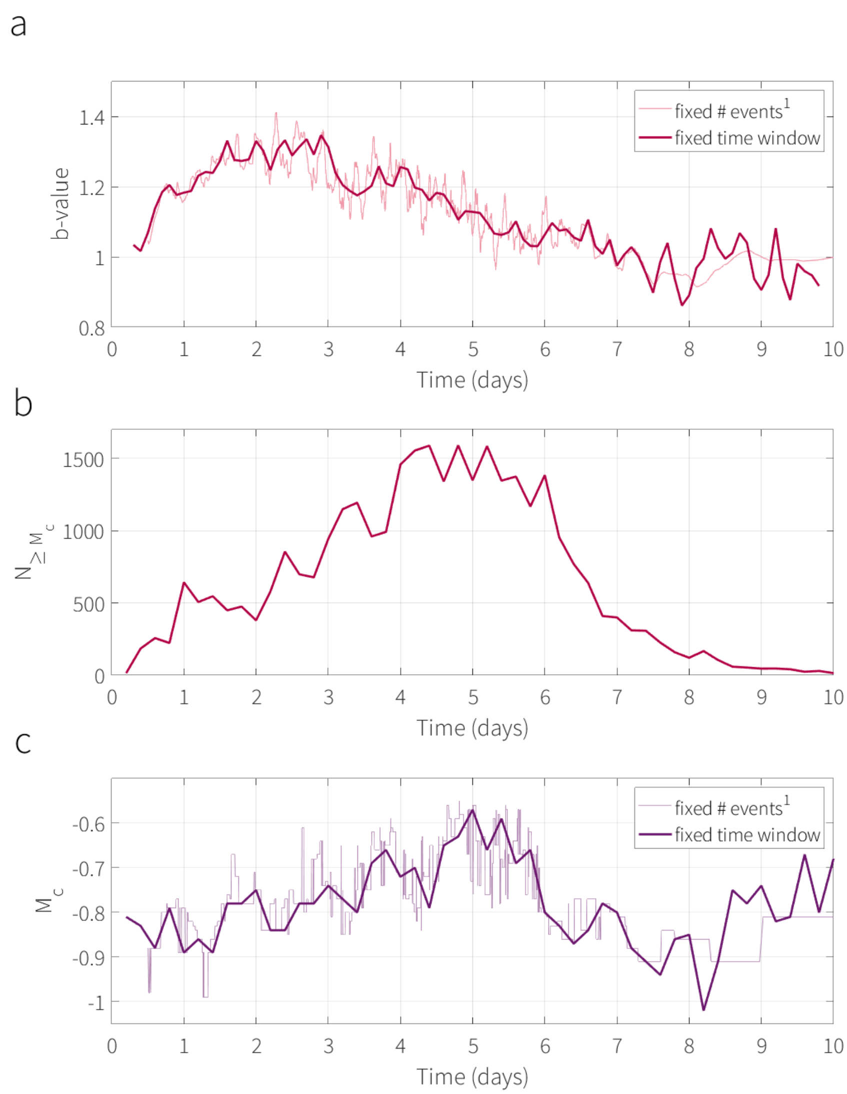

Figure S1. High resolution template-matched catalogue of Herrmann et al.[1] a) b-value with fixed number of events[1] and with fixed time window b) Hourly normalised number of events above completeness observed in Basel using the 0.2 day binning. c) Magnitude of completeness with the fixed number of event and fixed time windows

Data accompanying Figure 1-a

Compilation of a-values, b-values, maximum observed magnitudes, magnitudes of completeness and injected volumes for different operational EGS and scientific injections. For Figure 1-a, the local magnitudes are converted to moment magnitude using Equation S1; and duration magnitudes converted to moment using Equation S2. This generic conversion is done to compare the sites but can introduce errors in the magnitude distribution depending on the specificities of the local and duration magnitude scales used for the sites.

$$M_w = \frac{2}{3} M_l + 0.833 \tag{S1}$$

$$M_w = 0.93 M_d + 0.35 \tag{S2}$$

Table S1. Figure 1a: a- and b-values observed in Geothermal systems and other injection operations

Site (Country, year)	$N \geq M_c$	**b-value**	**Mmax(obs)**	**Mc**	$V_{tot}(m^3)$	**Type**	**Reference**
KTB (Germany, 1994)	54	0.93	1.2	-1.3 M_L	86	Scientific	Disnke & Shapiro, 2013[2]
Soultz-sous-Forêts (France, 2000)	7062	1.29	2.6	0.4 M_d	2.34e4	EGS	Cuenot et al., 2008[3]
Basel GEL catalogue (Switzerland, 2006)	2313	1.65	3.4	1.0 M_L	1.08e4	EGS	Häring et al., 2008[4]
Basel templated catalogue (Switzerland, 2006)	164385	1.33	3.14	-0.7 M_w	1.08e4	EGS	Herrmann et al., 2019[1]
Helsinki (Finland, 2018)	43882	1.26	1.9	-1.21 M_w	1.816e4	EGS	Kwiatek et al., 2019[5]
Grimsel HS4 (Switzerland, 2017)	919	1.36	-2.76	-4.3 $M_{l_{corr}}$	1.277	Scientific	Villiger et al., 2020[6]
Pohang (South Korea, 2017)	122	0.65	5.5	-0.4 M_w	1.28e4	EGS	Woo et al., 2019[7]
Bedretto ST1 (Switzerland, 2020)	500	2.95	-2.24	-2.82 M_w	602	Scientific	Hertrich et al., 2021[8]
Bedretto ST2 (Switzerland, 2020)	861	2.23	-1.71	-3.01 M_w	220	Scientific	Hertrich et al., 2021[8]

Complement to Figure 2

Complement to Figure 2-d and -f

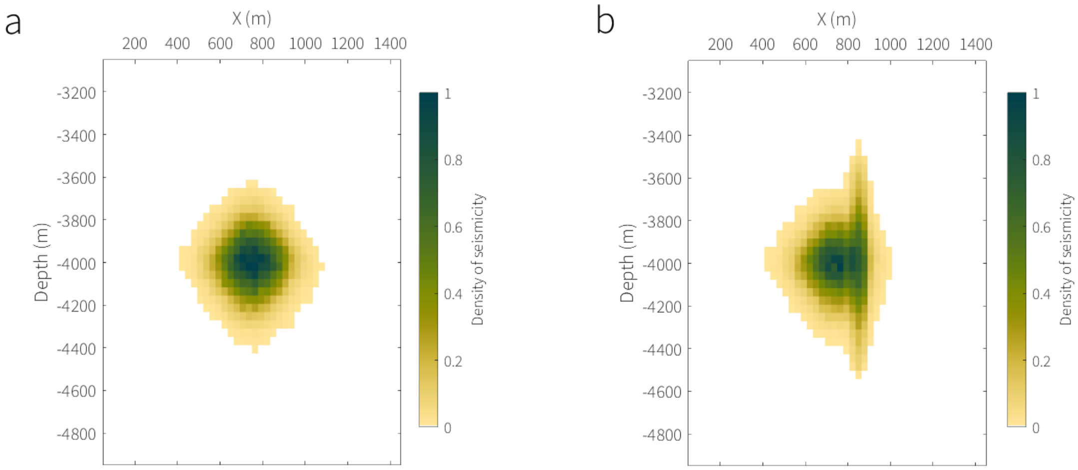

Figure S2. Vertical map of the density of the seismicity averaged over all realisations without a fault (a) and with a fault (b)

Spatio-temporal distribution of the seismicity

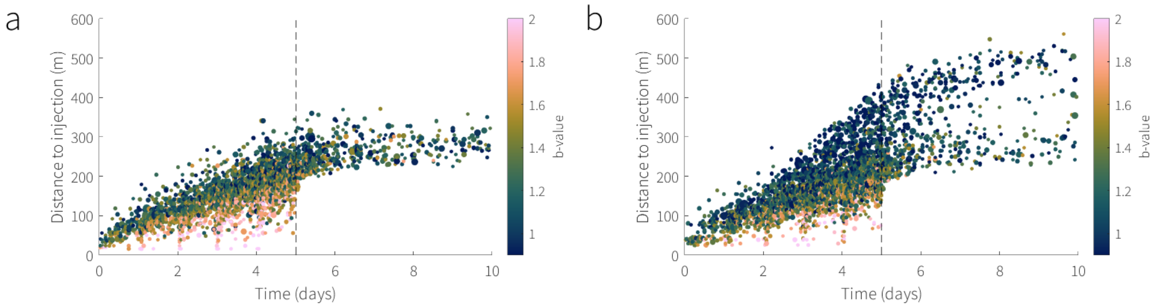

Figure S3. Distance-time (RT) plot for one realisation of the base case without a fault (a) and with a fault (b); the size of the dots is proportional to the magnitude of the events, the color of the dots denotes the b-value assigned to the reactivated seed.

Spatio-temporal distribution of the b-value at different times

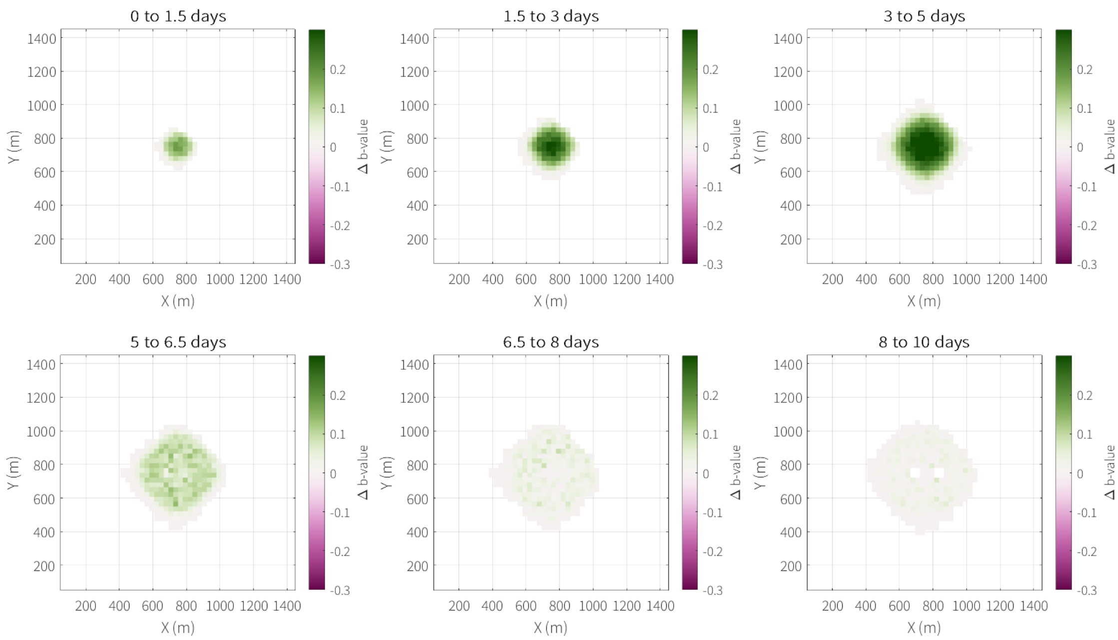

Figure S4. No fault case - Spatial distribution of the change in b-value (averaged over all realisations) at different times, the "0" reference corresponds to the initial rock/stress properties.

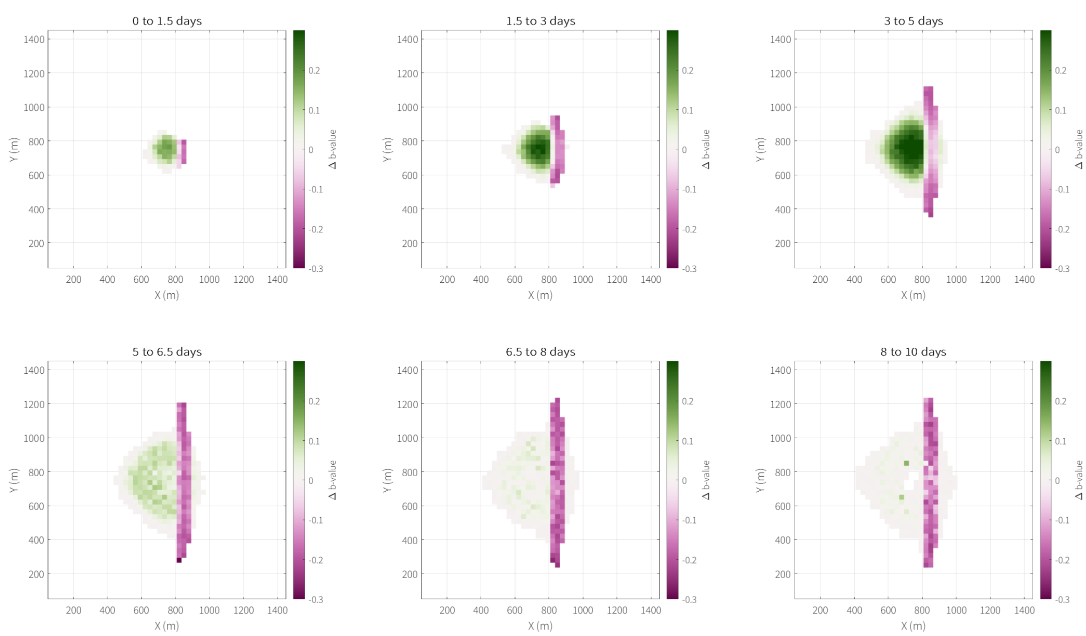

Figure S5. Fault case - Spatial distribution of the change in b-value (averaged over all realisations) at different times. To highlight the fault the changes in b-value are computed with the non-fault rock/stress properties as reference.

Complement to Figure 3

Decomposition of the cumulative probability of occurrence of a magnitude 3.5 for the base case with every single stochastic realisation (thin lines) and the average preferred response (thick line) for b-value, a-value, probability of occurrence and cumulative probability of occurrence.

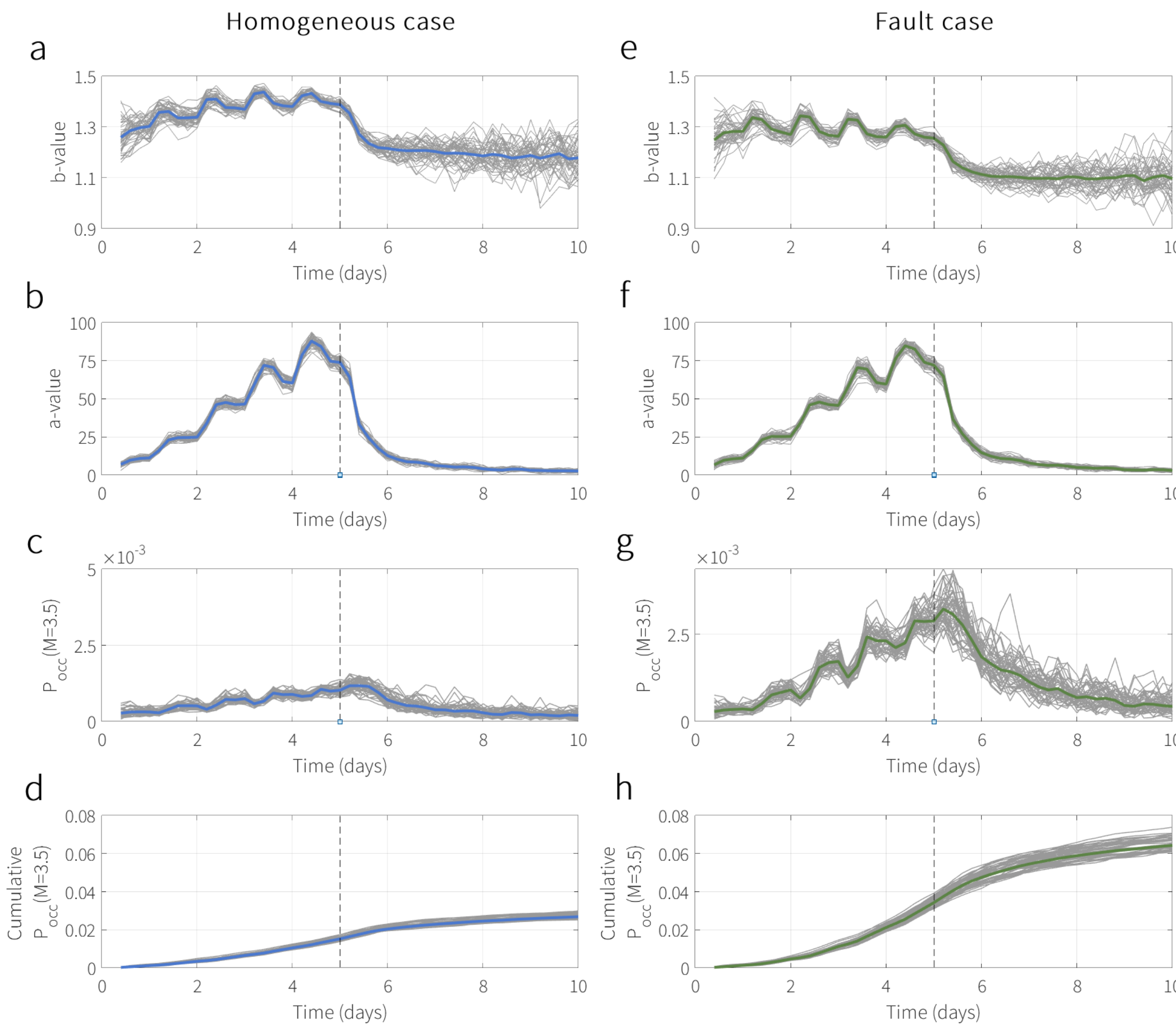

Figure S6. Homogeneous base case a) b-value at 0.2 days intervals b) hourly a-value at 0.2 days interval c) probability of occurrence of a magnitude greater or equal to 3.5 d) cumulative probability of occurrence of a magnitude greater or equal to 3.5. Fault case e) b-value at 0.2 days intervals f) hourly a-value at 0.2 days interval g) probability of occurrence of a magnitude greater or equal to 3.5 h) cumulative probability of occurrence of a magnitude greater or equal to 3.5.

Influence of the total injected volume

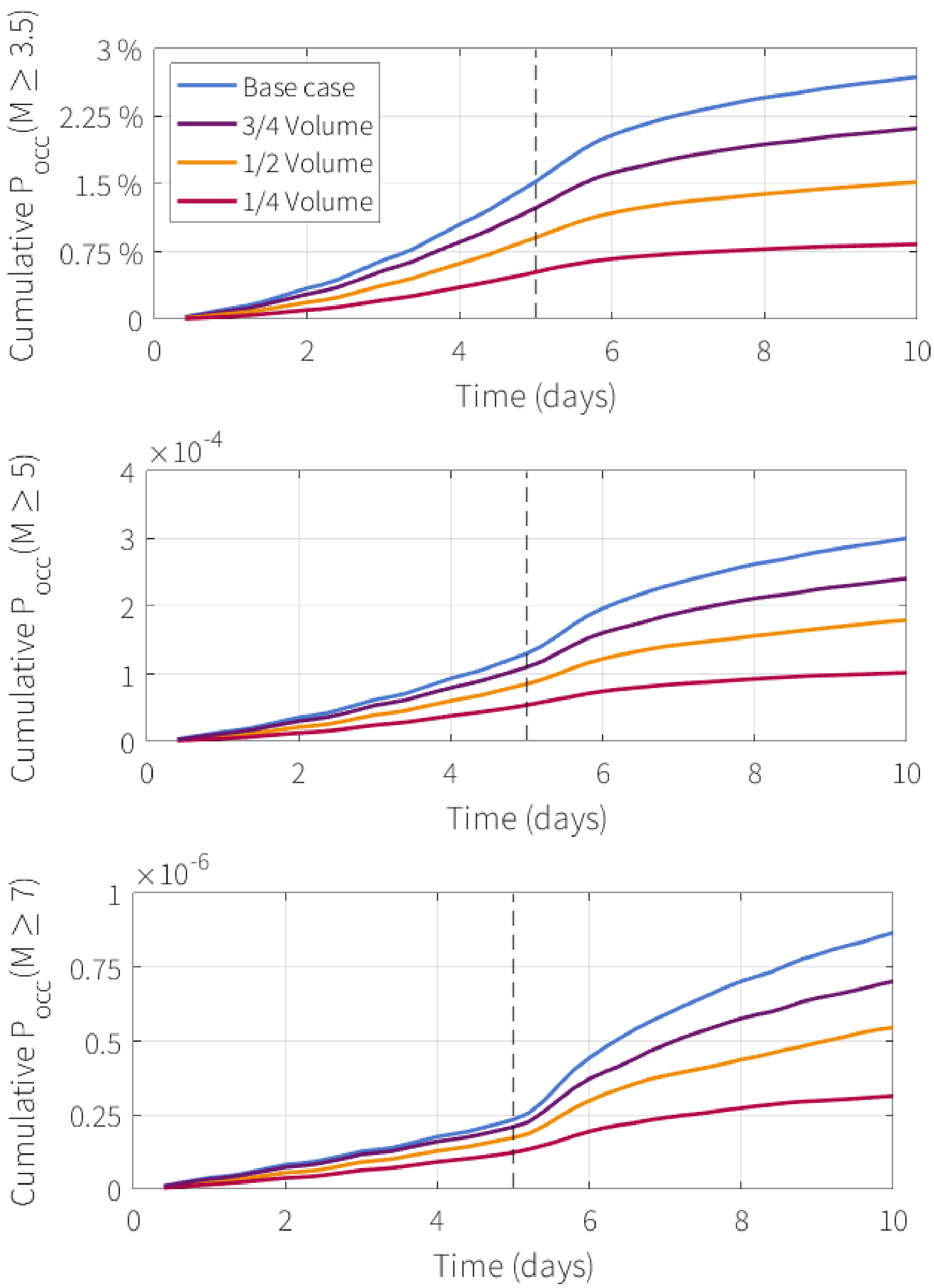

Figure S7. Cumulative probability of occurrence of a magnitude greater or equal to 3.5 (a), 5 (b) and 7 (c) for the base case without fault and fractions of the base case injected volume

Complement to Figure 6 with higher magnitudes

Similar to Figure 6 for magnitudes 5 and 7 both with (dashed lines) and without fault (solid lines) for all injection strategies.

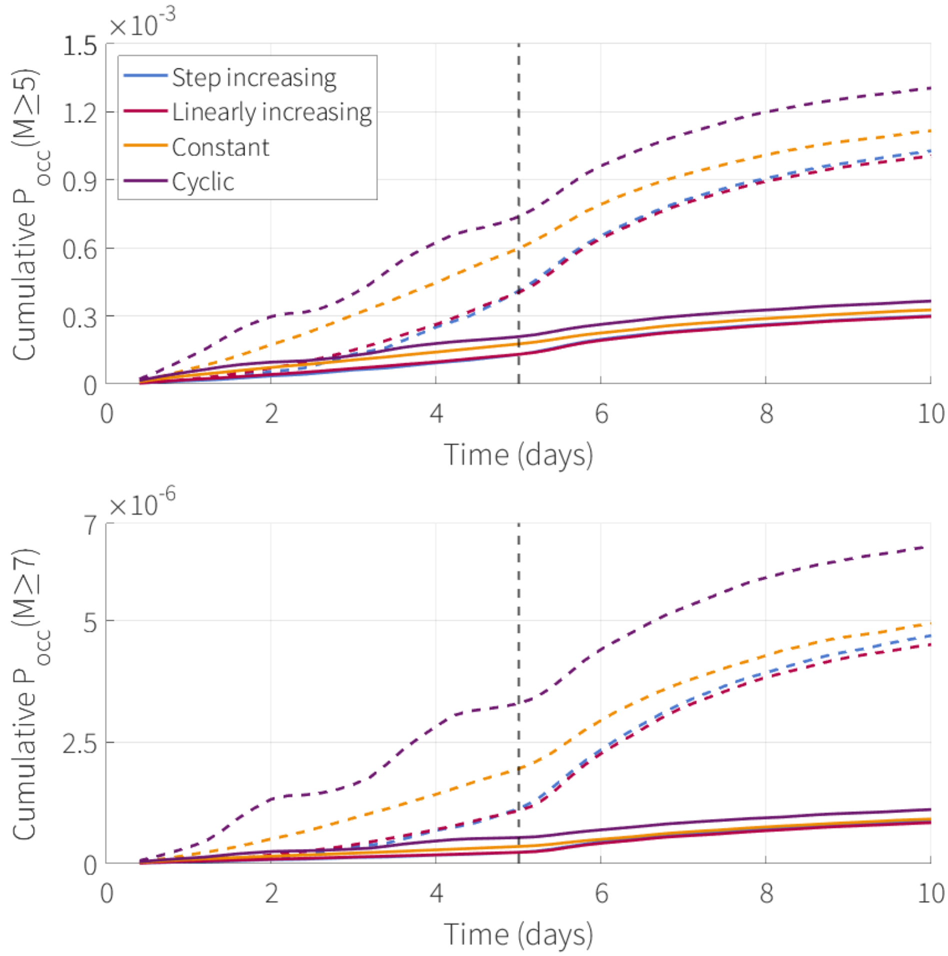

Figure S8. Cumulative probability of occurrence of a magnitude 5 (top) and 7 (bottom) event for the different injection strategies. The solid lines correspond to the homogeneous cases and the dashed lines to the cases with a fault

Influence of the number of stochastic realisations

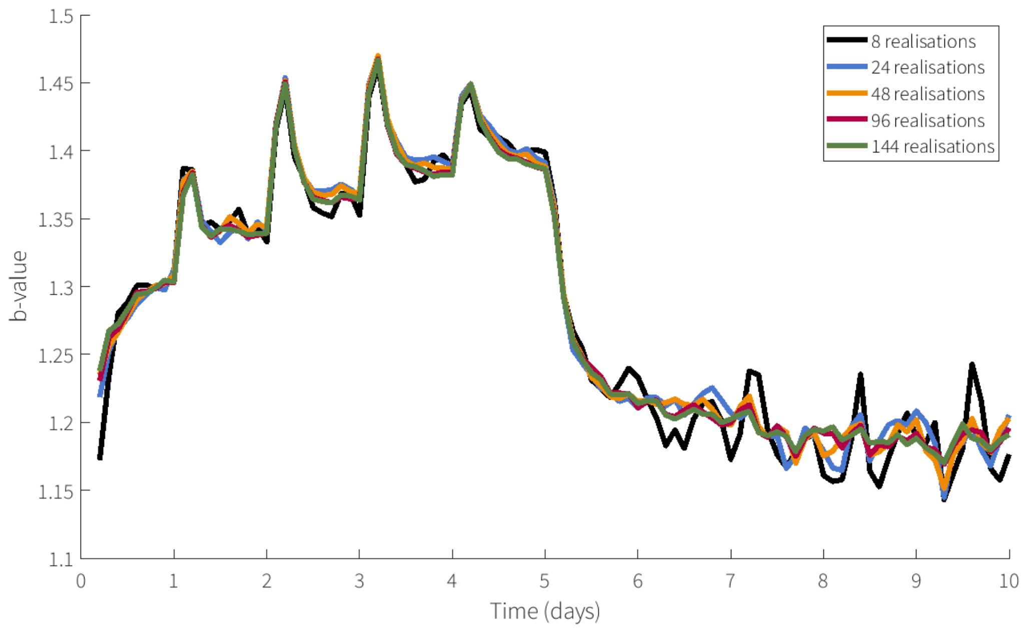

Figure S9. Step-increasing injection: temporal evolution of the b-value with different numbers of stochastic realisations

Stress drop and differential stress modelling

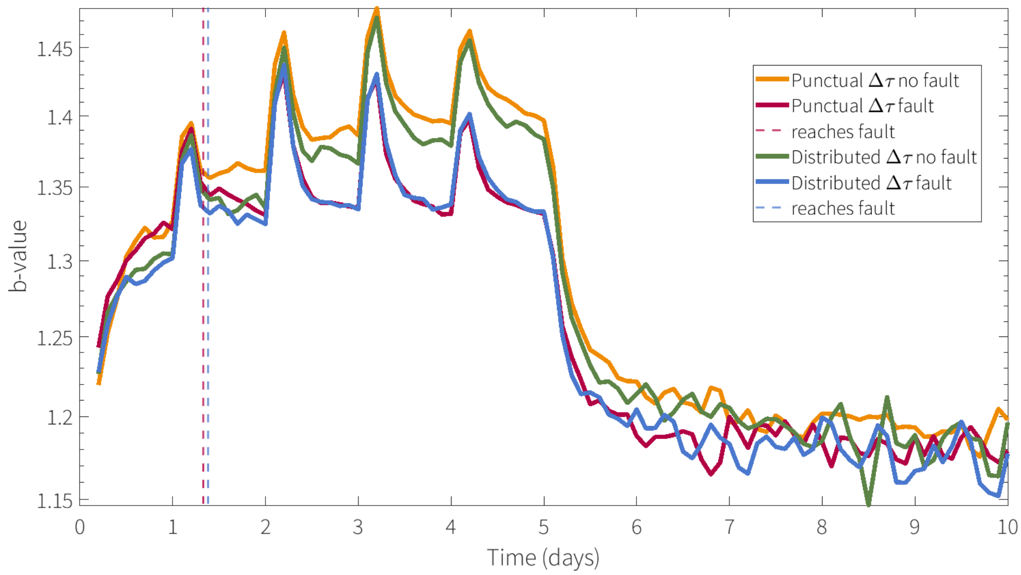

Figure S10. Step-increasing injection: temporal evolution of the b-value with different implementations of the stress drop (punctual or distributed) both with and without fault (colour-coded)

Fault build-up

Detail of the steps of construction of a seismogenic hydraulic fault.

Table S2. Average number of events and b-value change between co-injection and natural state of the system for each step of the fault build-up (fault of permeability $k = 10^{-15} m^2$, placed 100 m from the injection

	$\bar{N}$	Δb
Homogeneous case	3258	0.2024
Hydraulic fault	3546	0.1829
Hydraulic fault low b-value	3303	0.1809
Hydraulic fault with low b-value and μ	3070	0.1804

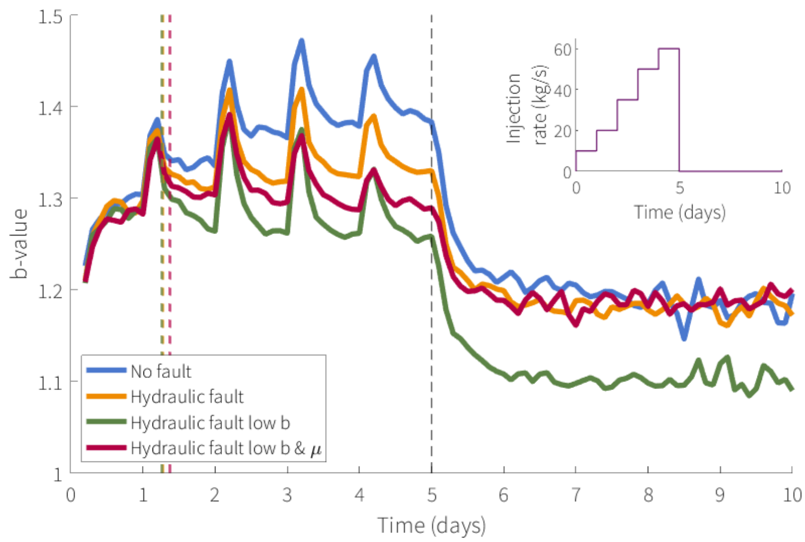

Figure S11.1. Step-increasing injection: temporal evolution of the b-value with different level of complexity of the fault (fixed time-window 0.2:0.1 days). The dashed line denotes when the fault gets reactivated in each case (colour-coded)

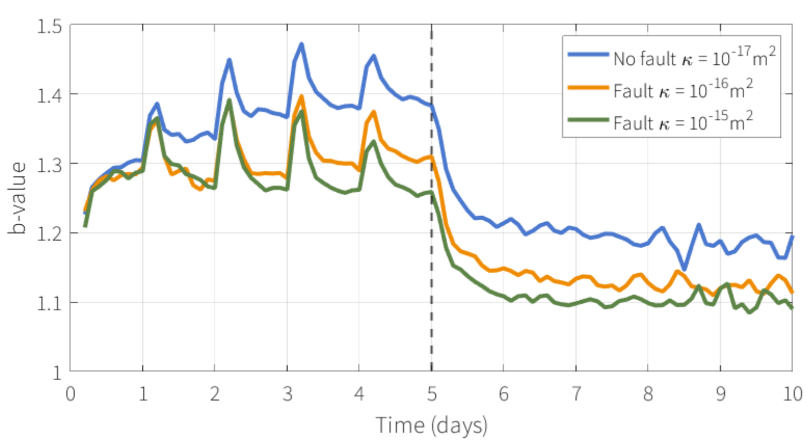

Figure S11.2. Step-increasing injection: temporal evolution of the b-value with different permeabilities of the fault (fixed time-window 0.2:0.1 days).

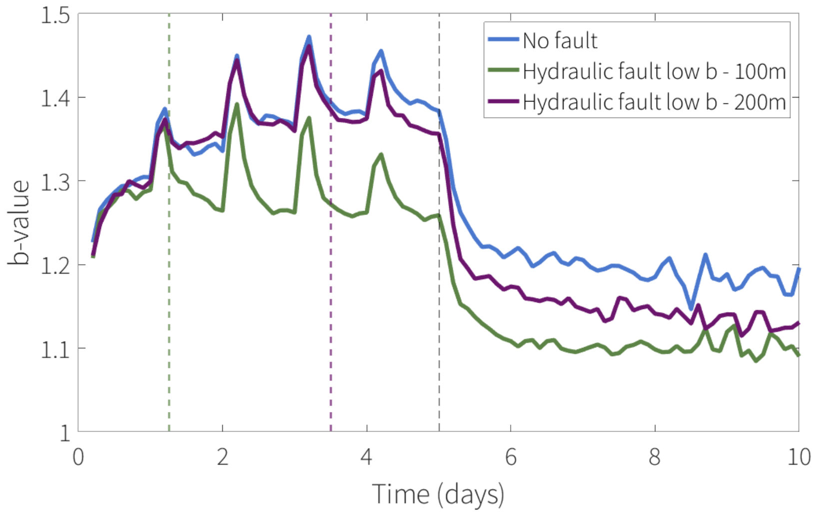

Figure S11.3. Step-increasing injection: temporal evolution of the b-value with the fault at different distances (fixed time-window 0.2:0.1 days).

Uncertainty on the transient b-value

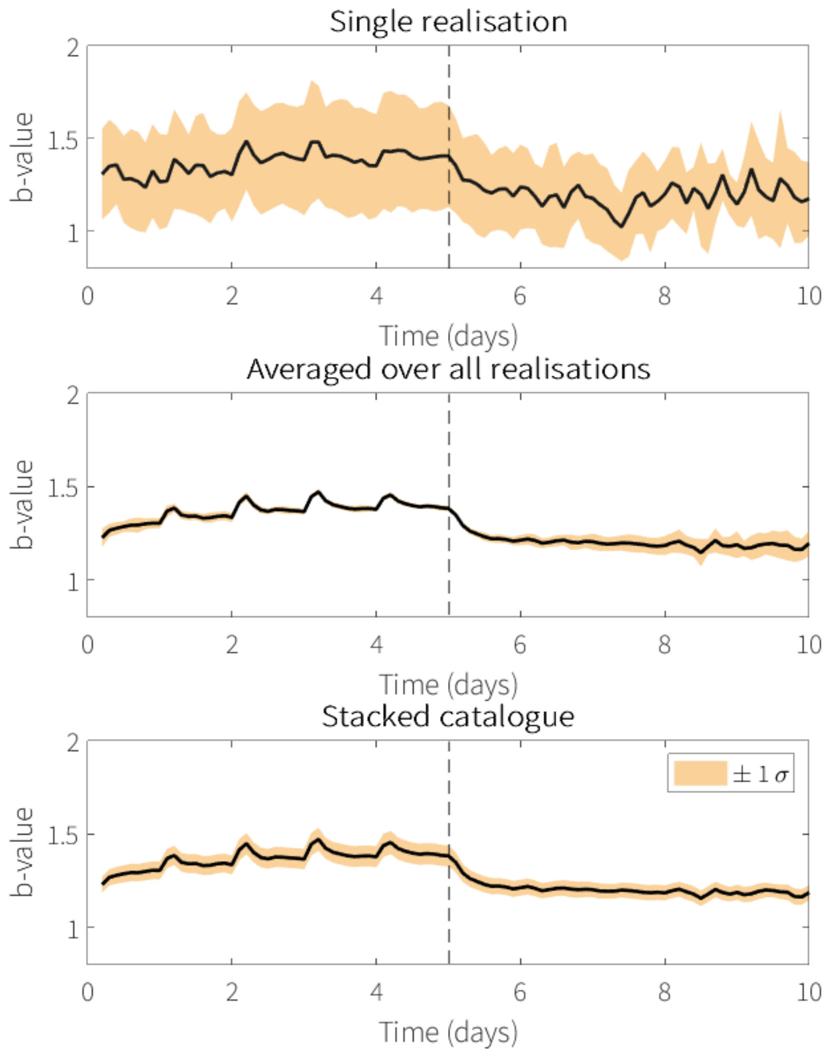

Figure S12. Base case - transient b-value and associated uncertainty at $\pm 1\sigma$ a) One realisation (randomly selected). b) Average over all 48 realisations. c) Considering a unique catalogue consisting of all 48 catalogues stacked.

Supplementary References

1. Herrmann, M., Kraft, T., Tormann, T., Scarabello, L. & Wiemer, S. A Consistent High-Resolution Catalog of Induced Seismicity in Basel Based on Matched Filter Detection and Tailored Post-Processing. *J. Geophys. Res. Solid Earth* **124**, 8449–8477, DOI: 10.1029/2019JB017468 (2019).
2. Dinske, C. & Shapiro, S. A. Seismotectonic state of reservoirs inferred from magnitude distributions of fluid-induced seismicity. *J. seismology* **17**, 13–25 (2013).
3. Cuenot, N., Dorbath, C. & Dorbath, L. Analysis of the microseismicity induced by fluid injections at the EGS site of Soultz-sous-Forêts (Alsace, France): Implications for the characterization of the geothermal reservoir properties. *Pure Appl. Geophys.* **165**, 797–828, DOI: 10.1007/s00024-008-0335-7 (2008).
4. Häring, M. O., Schanz, U., Ladner, F. & Dyer, B. C. Characterisation of the Basel 1 enhanced geothermal system. *Geothermics* **37**, 469–495, DOI: 10.1016/j.geothermics.2008.06.002 (2008).
5. Kwiatek, G. *et al.* Controlling fluid-induced seismicity during a 6.1-km-deep geothermal stimulation in Finland. *Sci. Adv.* **5**, 1–12, DOI: 10.1126/sciadv.aav7224 (2019).
6. Villiger, L. *et al.* Influence of reservoir geology on seismic response during decameter-scale hydraulic stimulations in crystalline rock. *Solid Earth* **11**, 627–655, DOI: 10.5194/se-11-627-2020 (2020).
7. Woo, J. U. *et al.* An In-Depth Seismological Analysis Revealing a Causal Link Between the 2017 MW 5.5 Pohang Earthquake and EGS Project. *J. Geophys. Res. Solid Earth* **124**, 13060–13078, DOI: 10.1029/2019JB018368 (2019).
8. Hertrich, M. *et al.* Characterization, hydraulic stimulation, and fluid circulation experiments in the Bedretto Underground Laboratory for Geosciences and Geoenergies. *55th U.S. Rock Mech. / Geomech. Symp. 2021* **4** (2021).